

## Catalytic Synthesis of Carbon Nanotubes using CeFeMgO: Study their Efficiency and Structural Insights

D. MANIKANDAN<sup>1</sup>, T. SOMANATHAN<sup>1,\*</sup> and A. PANDURANGAN<sup>2</sup>

<sup>1</sup>Department of Chemistry, School of Basic Sciences, Vels Institute of Science, Technology and Advanced Studies, Chennai-600117, India

<sup>2</sup>Department of Chemistry, Anna University, Chennai-600025, India

\*Corresponding author: E-mail: soma.sbs@vistas.ac.in

Received: 6 December 2024;

Accepted: 15 January 2025;

Published online: 31 January 2025;

AJC-21893

The catalytic synthesis of carbon nanotubes (CNTs) using CeFeMgO catalysts represents a promising avenue for achieving efficient and controlled carbon nanotube growth. The CeFeMgO catalysts were prepared by solution combustion techniques and the growth of CNTs was obtained from the chemical vapour deposition (CVD) method. The X-ray diffraction (XRD), high-resolution scanning electron microscopy (HR-SEM), energy dispersive X-ray spectroscopy (EDAX), transmission electron microscopy (TEM), thermogravimetric analyzer (TGA), BET, particle size distribution, were employed to characterize the morphology, crystallinity and composition of the synthesized CNTs. Results indicate that the study reveals the robust catalytic activity that facilitates the formation of high-quality carbon nanotubes (CNTs), highlighting the efficiency of CeFeMgO catalysts in promoting CNT growth and elucidating the structural aspects crucial for optimizing carbon nanotube production. The results demonstrate uniform carbon nanotube dimensions, excellent crystallinity and minimal defects, highlighting the efficacy of catalyst in achieving controlled and efficient carbon nanotube synthesis. This study enhances the comprehension and utilization of CeFeMgO catalysts in the synthesis of carbon nanomaterials.

**Keywords:** Multiwalled carbon nanotubes, Chemical vapour deposition, CeFeMgO catalyst, Solution combustion techniques.

### INTRODUCTION

Carbon nanotubes (CNTs) continue to be of significant interest due to their unique mechanical, electrical and thermal properties, which make them invaluable for a wide range of applications, from nanocomposites to electronics and energy storage [1]. The development of efficient and scalable methods for CNT synthesis remains a key challenge in the field. Among the various techniques employed for CNT production, catalytic chemical vapour deposition (CCVD) stands out as one of the most promising due to its ability to produce high-quality CNTs under relatively mild reaction conditions [2]. The performance of CCVD largely depends on the choice of catalysts, which play a critical role in determining the yield, structure and quality of the CNTs.

Recent advancements in catalyst design have led to the exploration of novel catalyst systems that offer enhanced efficiency and selectivity in CNT growth [3]. Metal oxide catalysts, particularly those containing transition metals and rare-earth

elements, have shown significant potential. Cerium oxide known for its excellent oxygen storage and release capacity, enhances the dissociation of carbon precursors and promotes the formation of active catalytic sites [4]. Iron oxide serves as a primary catalyst for the decomposition of carbon containing precursors, facilitating the nucleation and growth of CNTs [5]. Magnesium oxide provides thermal stability and helps prevent sintering of active sites, thereby improving catalyst longevity and ensuring consistent CNT production. The combination of these oxides develops a synergistic effect that not only improves the catalytic efficiency but also provides better control over the size, morphology and structural integrity of the CNTs produced [6-8].

Thus, considering the above facts, the catalysts composed of cerium, iron and magnesium, such as CeFeMgO may emerge as a promising catalyst system for the synthesis of CNTs. In this study, we investigate the catalytic performance of CeFeMgO (CFMO) for the CNT synthesis, focusing on the efficiency of the process, the structural characteristics of the CNTs and the role of the catalyst components in influencing the growth mech-

anism. This research aims to provide insights into the fundamental interactions between the catalyst components and their impact on CNT formation as well as to identify strategies for optimizing the synthesis conditions to improve yield and quality.

## EXPERIMENTAL

All analytical grade chemicals such as cerium nitrate hexahydrate [ $\text{Ce}(\text{NO}_3)_3 \cdot 6\text{H}_2\text{O}$ ], iron nitrate hexahydrate [ $\text{Fe}(\text{NO}_3)_3 \cdot 6\text{H}_2\text{O}$ ] and magnesium nitrate hexahydrate [ $\text{Mg}(\text{NO}_3)_2 \cdot 6\text{H}_2\text{O}$ ] used for the synthesis of CeFeMgO catalyst were purchased from Sigma-Aldrich, USA. Hydrogen gas (99.99%), nitrogen gas (99.99%) and acetylene gas utilized for the synthesis of carbon nanotubes (CNTs) were purchased from Indogas Private Limited, Chennai, India.

**Characterization:** The X-ray powder diffractograms of calcined catalysts and purified CNT samples were obtained on a Rigaku SmartLab high-resolution X-ray diffractometer equipped with a liquid nitrogen cooled germanium solid-state detector using  $\text{CuK}\alpha$  radiation. The  $\text{N}_2$  adsorption-desorption isotherms were measured at  $-197^\circ\text{C}$  using a Micromeritics ASAP 2000. Prior to the experiments, the samples were dried at  $130^\circ\text{C}$  and left for 8 h in flowing argon at a flow rate of 60 mL/min at  $200^\circ\text{C}$ . The morphology and chemical composition were analyzed with FESEM-EDX using Thermo-Fisher Scientific instrument. To determine the particle size and structure of the CNTs, a JEOL Japan JEM-2100 Plus instrument was used in a high-resolution transmission electron microscope (HR-TEM). Raman spectra were recorded with a Micro-Raman system RM 1000 Renishaw using a laser excitation line at 532 nm (Nd-YAG).

**Synthesis of CeFeMgO (CFMO) catalyst:** According to previous investigations [6,9], in this study, the synthesis of CFMO catalyst was carried out using solution combustion method. Dissolved the appropriate stoichiometric amounts of cerium(III) nitrate [ $\text{Ce}(\text{NO}_3)_3$ ], ferrous nitrate [ $\text{Fe}(\text{NO}_3)_3$ ] and magnesium nitrate [ $\text{Mg}(\text{NO}_3)_2$ ] in deionized water with a molar ratio of  $\text{Ce}_{0.1}\text{Fe}_{0.24}\text{Mg}_{0.66}\text{O}$ . Stirred the solution thoroughly to ensure complete dissolution of the salts and added citric acid (2 g) as foaming and combustion ingredient. Then transferred the solution to a crucible or ceramic dish and heat it in a muffle furnace or a hotplate under controlled conditions and heated at  $550^\circ\text{C}$  for 5 min. Upon completion of the combustion process, the product was calcinated at higher temperatures (between  $600^\circ\text{C}$  and  $800^\circ\text{C}$ ) in air to eliminate any remaining organic material and to guarantee the development of a crystalline metal oxide structure. The final CFMO catalyst can be characterized by various techniques to confirm its composition, structure and surface area utilizing X-ray diffraction (XRD), scanning electron microscope and BET surface area analyzer.

**Catalytic growth of helical CNTs:** The synthesis of helical CNTs using CFMO combustion catalysts involves a well-controlled CCVD process. A single step for the catalytic growth of helical CNTs was utilized. Transferred the CFMO catalyst into a tube furnace or a quartz reactor with a controlled gas flow system and then heated the CeFeMgO catalyst in the presence of  $\text{N}_2$  (200 mL/min) and  $\text{H}_2$  (100 mL/min) at  $600\text{--}700^\circ\text{C}$ . The catalyst activation ensures the formation of active sites on the surface of the CFMO, where the carbon precursor will

decompose and initiate CNT growth. Once the catalyst was activated, introduce the carbon source (acetylene, 20 mL/min) into the furnace. The decomposition of acetylene at high temperature results in the formation of carbon species, which will nucleate and grow on the CFMO catalyst particles, forming CNTs. To achieve the helical CNTs, it is crucial to maintain specific reaction parameters, such as the temperature, gas flow rate and catalyst concentration. The synthesized CNTs may contain impurities or amorphous carbon. These can be removed by washing the CNTs with deionized water or mild acid (*e.g.* HCl) followed by drying.

## RESULTS AND DISCUSSION

### Characterization of CFMO catalyst

**XRD studies:** The XRD pattern of a CFMO catalyst (Fig. 1) provides valuable information about the crystallographic phases, crystallinity and particle size of the catalyst components, including cerium oxide ( $\text{CeO}_2$ ), iron oxide ( $\text{Fe}_2\text{O}_3$  or  $\text{Fe}_3\text{O}_4$ ) and magnesium oxide ( $\text{MgO}$ ). These phases play a crucial role in the catalytic activity of the material, particularly for reactions like carbon nanotube (CNT) growth.  $\text{CeO}_2$  typically exhibits a cubic symmetry. The most prominent XRD peaks are observed at  $28.5^\circ$  (111),  $33.2^\circ$  (200),  $47.4^\circ$  (220),  $56.4^\circ$  (311). These peaks indicate the presence of  $\text{CeO}_2$  in its most stable phase, which is crucial for promoting oxygen storage and enhancing the redox properties of catalyst. The peaks observed at  $33.2^\circ$  (110),  $43.0^\circ$  (400) and  $57.2^\circ$  (511) represent the iron oxide phases  $\text{Fe}_2\text{O}_3$  and  $\text{Fe}_3\text{O}_4$ , respectively. Thus, confirmed iron oxide phases that act as active sites for CNT growth.  $\text{MgO}$  similarly displays distinct peaks at  $42.9^\circ$  (111),  $62.4^\circ$  (200), and  $78.6^\circ$  (311), reflecting its cubic symmetry and indicating high crystallinity, which enhances the stability of catalyst and prevents sintering. In CFMO catalysts, the XRD pattern often shows overlapping or broad peaks, indicating the presence of mixed metal oxides or solid solutions. These phases enhance the synergistic catalytic behaviour, improving the overall activity and selectivity during CNT synthesis [1,6,10].

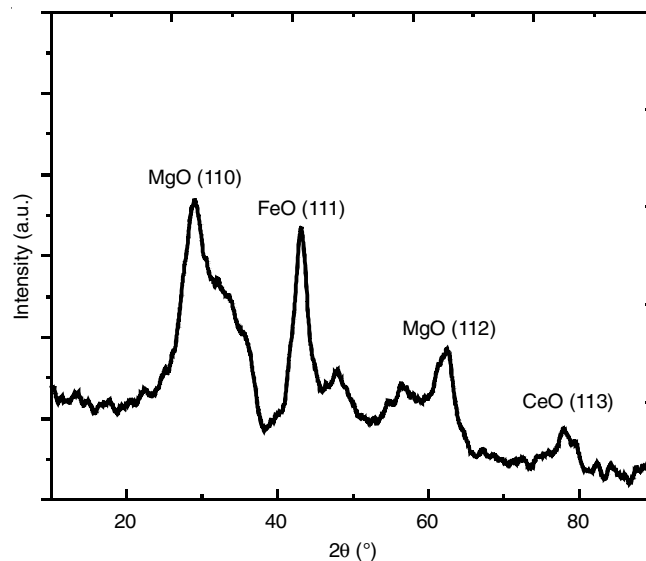


Fig. 1. XRD pattern of CFMO catalyst

**Nitrogen adsorption–desorption isotherms:** The  $N_2$  adsorption-desorption isotherm of CFMO catalysts provides critical information about the textural properties such as surface area, pore size distribution and pore volume. A Type-IV isotherm indicates the presence of mesopores (pore diameter between 2 and 50 nm). Low  $P/P_0$  region ( $< 0.1$ ) of the isotherm typically shows a steep increase in the nitrogen adsorption at low relative pressures, which corresponds to the monolayer adsorption on the surface of the catalyst and used to calculate the BET surface area. Intermediate  $P/P_0$  region (0.1-0.9) of the isotherm may exhibit a Type-IV pattern with a hysteresis loop indicating mesoporosity which clearly seen in Fig. 2. The loop suggests the presence of mesopores that are accessible to nitrogen molecules during adsorption and desorption. High  $P/P_0$  region ( $> 0.9$ ) of the nitrogen adsorption at higher relative pressures corresponds to the filling of macropores and provides information about the total pore volume of the catalyst (Table-1).

TABLE-1 TEXTURAL PROPERTIES OF CFMO CATALYST			
CFMO at 150 °C	Surface area ( $m^2 g^{-1}$ )	Pore volume ( $cc^3 g^{-1}$ )	Pore size (nm)
	14.9507	0.995	8.5967

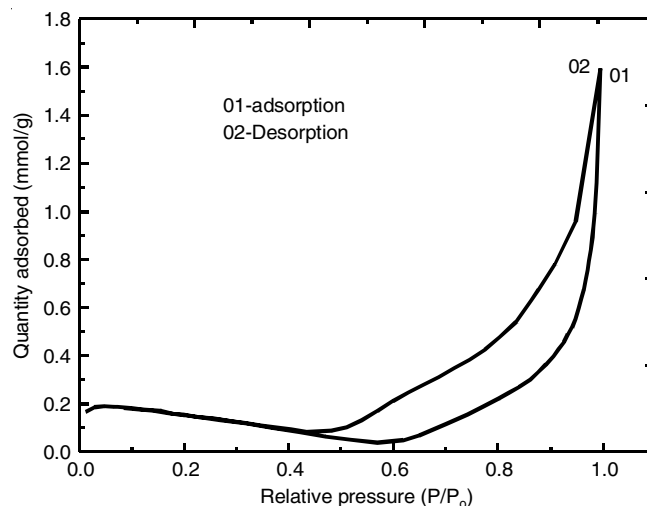


Fig. 2. Nitrogen adsorption-desorption isotherms of CFMO catalyst

**HR-SEM studies:** The high-resolution SEM images revealed the particle size and morphology of the CFMO catalyst (Fig. 3a). The particles were observed to be relatively uniform in size, indicating good dispersion, which is essential for maximizing the active surface area. The surface roughness and the

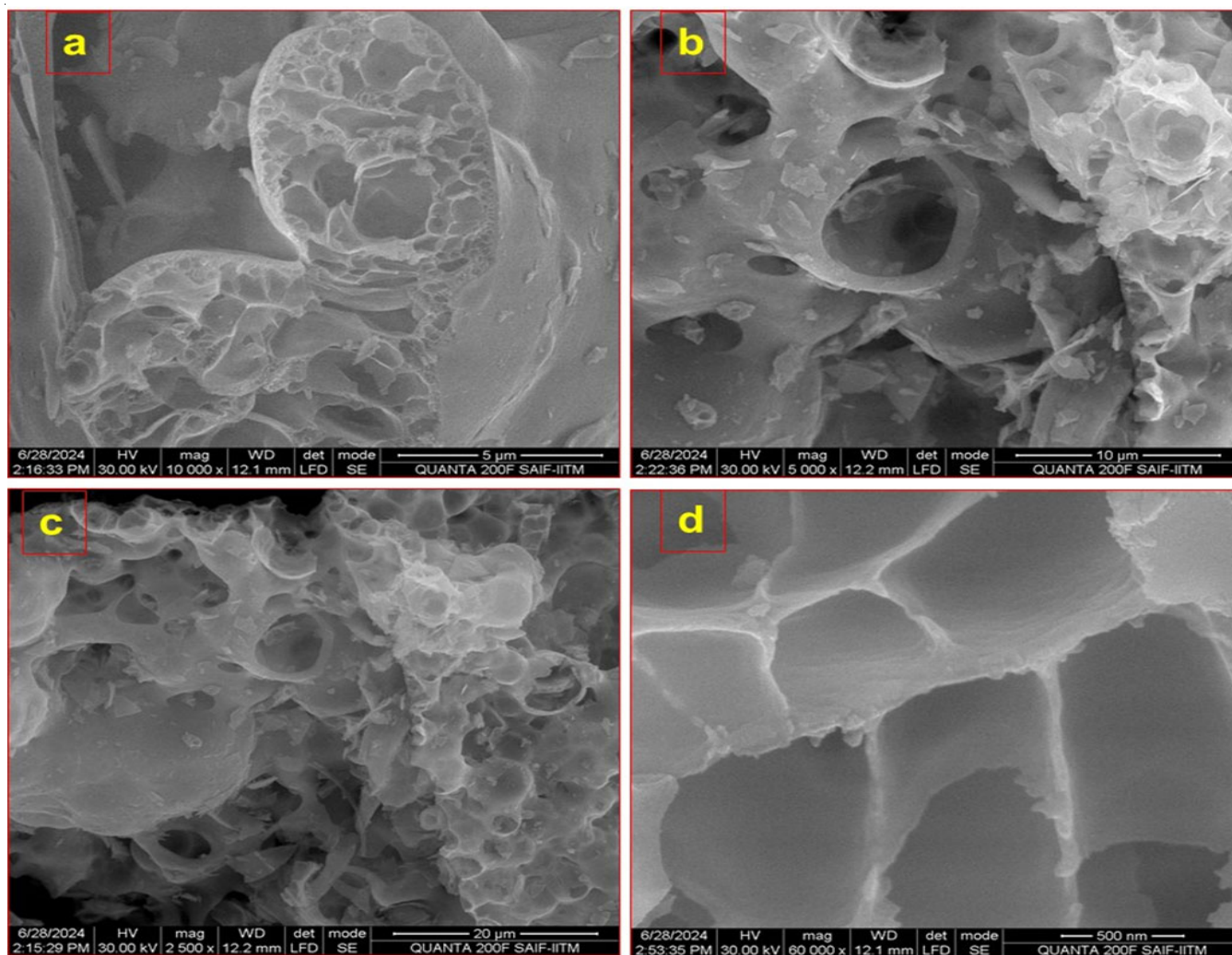


Fig. 3. HR-SEM analysis of the CFMO catalyst

presence of mesopores suggest that the catalyst has a well-developed porous structure (Fig. 3b-c), favourable for improving reactant accessibility and enhancing catalytic activity. No significant aggregation or sintering was observed, indicating good stability at the resolution imaged (Fig. 3d).

**EDAX studies:** Elemental analysis using EDAX showed that the catalyst contained the expected components cerium, iron, magnesium and oxygen with well-distributed concentrations of each element which is shown in Fig. 4. The Ce and Fe were found to be homogeneously distributed across the surface, suggesting good interaction between these two active components, which is crucial for optimizing redox properties and catalytic performance. The Mg content was uniformly distributed, assisting in the stabilization of the catalyst and inhibiting phase separation or sintering. The oxygen mapping revealed a steady presence throughout the surface, underscoring the material's ability for oxygen storage and release, an essential characteristic for the oxidative catalytic processes [11].

**Particle size analysis:** Particle size analysis of the CFMO catalyst [12] was performed using dynamic light scattering (DLS), a technique that measures the Brownian motion of particles suspended in a liquid to determine their hydrodynamic diameter. This method is particularly useful for characterizing the nanometer-sized particles in colloidal or dispersed systems, providing detailed information about the size distribution and polydispersity. The DLS analysis of the CFMO catalyst revealed a narrow particle size distribution, with the majority of particles having a hydrodynamic diameter ranging from 10 to 100 nm. The mean particle size (Z-average) was found to be approximately 45 nm, suggesting that the catalyst exists primarily as fine, dispersed nanoparticles in suspension. A relatively low polydispersity index (PDI) was observed, indicating that the particles are of relatively uniform size, which is desirable for maintaining consistent catalytic properties.

### Characterization of helical CNTs

**XRD studies:** A prominent feature of the XRD pattern for helical CNTs is the (002) peak, which represents the inter-

layer spacing (*d*-spacing) between the graphene sheets (Fig. 5). This peak generally appears around  $2\theta \approx 26^\circ$  and corresponds to a *d*-spacing of approximately 0.34 nm, characteristic of graphite and graphitic structures in the helical CNTs. Depending on the level of graphitization and the nature of the CNTs, there may also be weaker peaks appearing around  $2\theta \approx 43^\circ$  and  $54^\circ$ , corresponding to the (100) and (101) planes of graphite [13]. In case of helical CNTs, the peaks observed were broader when compared to those of hybrid CNTs, indicating a decrease in crystallite size attributed to the strain caused by the helical configuration. The broadening of the (002) peak could be more evident in hybrid CNTs than in straight CNTs, due to the twisted configuration potentially leading to an increase in defects and irregularities within the graphitic layers.

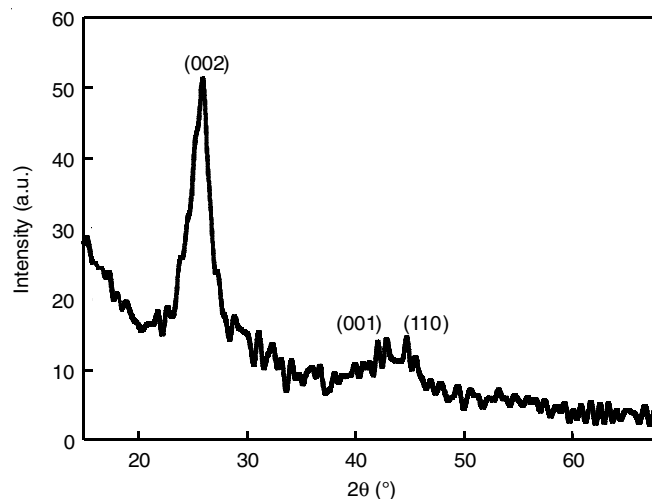


Fig. 5. XRD pattern of helical CNTs using CFMO catalyst

**Morphological studies:** The SEM images of helical CNTs grown with CFMO catalyst clearly exhibit the characteristic helical structure, with visible twisting along the axis of the nanotubes (Fig. 6). The helical nature is evident from the spiral-like curvature observed in the CNTs, confirming the successful

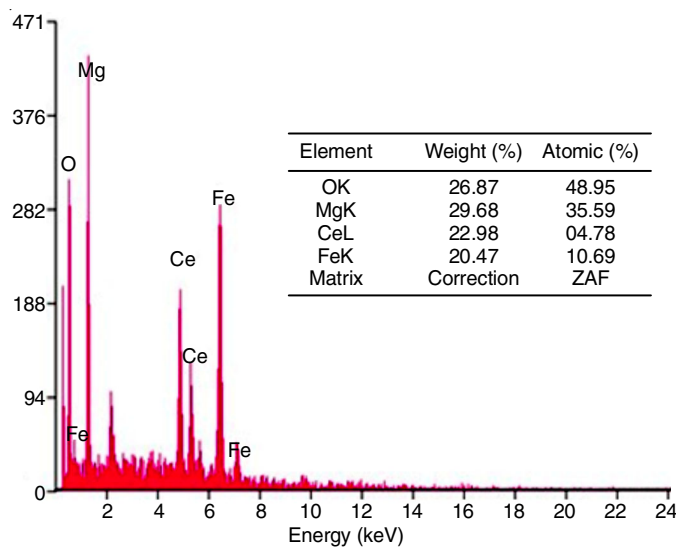
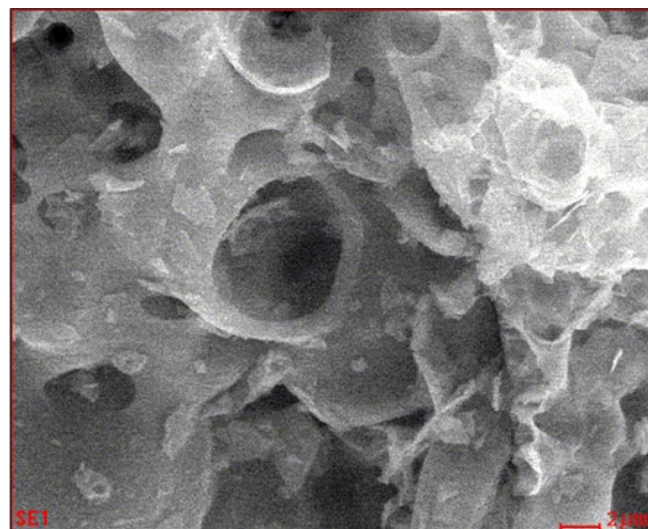


Fig. 4. EDAX analysis of the CFMO catalyst



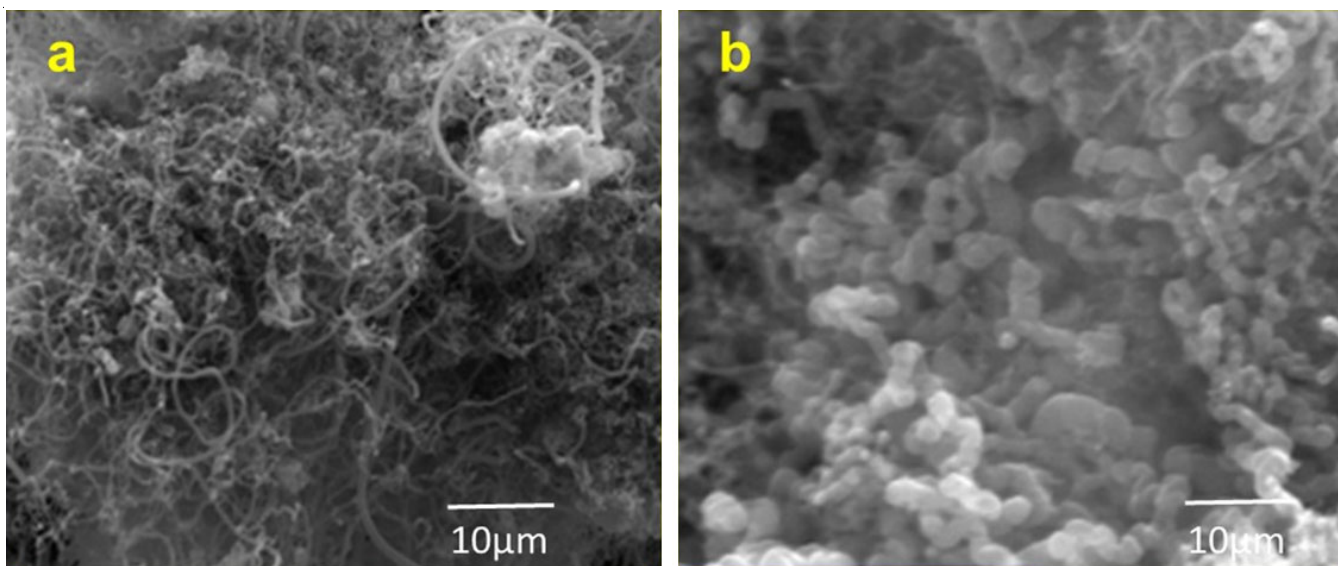


Fig. 6. SEM image of helical CNTs using CFMO catalyst

formation of helical CNTs rather than simple straight or multi-walled CNTs. The spiral pitch or the number of twists per unit length of the nanotube, appears consistent across different regions of the sample. The CFMO catalyst particles are visibly dispersed on the CNT surfaces, especially near the nanotube tips. These catalyst particles likely play a significant role in

the nucleation and growth of the CNTs and their presence suggests that the CFMO mixture acts as an effective catalyst in the CNT growth process [9].

The TEM images clearly show the helical structure of the CNTs (Fig. 7), which display a consistent spiral geometry along their length, with well-defined twists and turns. The pitch of

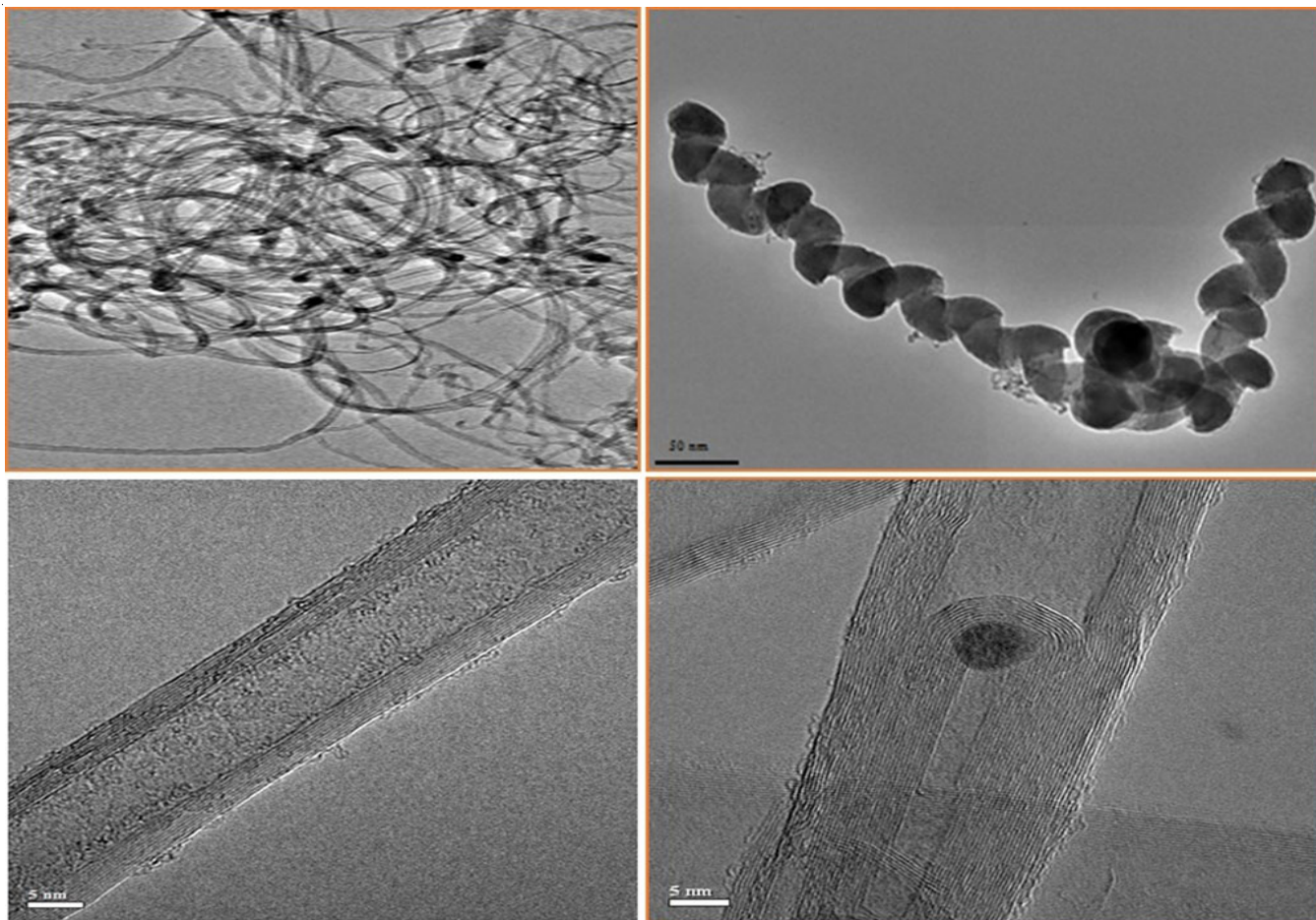


Fig. 7. TEM image of helical CNTs using CFMO catalyst

the helix (the number of twists per unit length) appears uniform, indicating a controlled growth process. The diameters of the helical CNTs range from approximately 20 to 50 nm, with the majority of the nanotubes exhibiting a uniform diameter. The twisted nature of the helical CNTs is clearly visible and the helical morphology is maintained throughout the length of nanotube. Catalyst particles from the CFMO mixture are visible at the tips and along the sidewalls of some of the nanotubes. These catalyst particles are relatively small and are dispersed evenly, suggesting good catalyst distribution during the CNT growth process [14].

**Raman spectral studies:** The synthesis of helical CNTs using a CFMO catalyst can influence these properties and the Raman spectrum serves as an effective method for characterizing these effects. The D-band, typically observed around  $1309\text{ cm}^{-1}$ , is associated with the disorder in the graphite-like structure of carbon [15]. It originates from the breathing mode of the carbon atoms in rings, which is activated by defects or disorder in the graphene structure. The G-band is located around  $1581\text{ cm}^{-1}$  and is the most prominent feature in the Raman spectrum of CNTs (Fig. 8). It corresponds to the  $E_{2g}$  phonon of  $sp^2$  carbon atoms, which reflects the in-plane vibration of the carbon atoms in the hexagonal lattice. It is a critical peak for distinguishing the single-walled CNTs (SWCNTs) from multi-walled CNTs (MWCNTs).

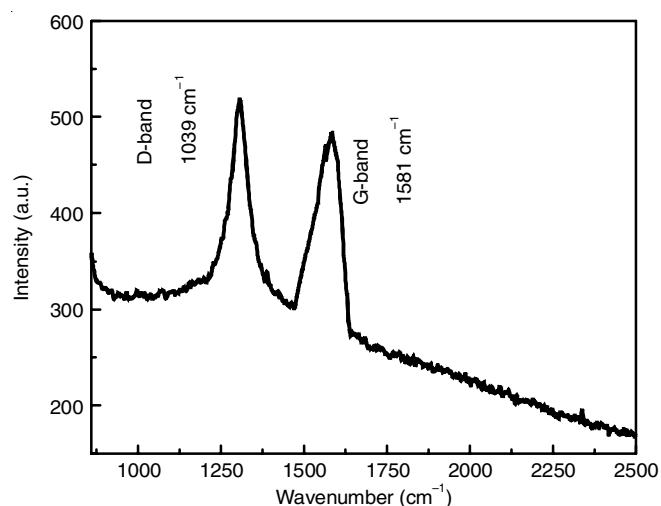


Fig. 8. Raman spectrum of helical CNTs using CFMO catalyst

## Conclusion

The catalytic synthesis of helical carbon nanotubes (CNTs) using CeFeMgO (cerium iron magnesium oxide) as a catalyst shows great promise for the efficient production of high-quality CNTs. The CFMO catalyst, with its unique combination of cerium, iron and magnesium, exhibits enhanced catalytic activity, stability and reusability compared to the conventional catalysts. The characterization results from XRD, SEM, TEM and Raman spectroscopy confirmed that this method produces

helical CNTs with excellent purity, uniformity and structural quality. These attributes make CeFeMgO a promising candidate for scalable, high-efficiency CNT production, with significant potential for applications in electronics, energy storage and advanced materials. Further research into the optimizing synthesis conditions and evaluating the catalyst's long-term stability will be crucial for its future industrial implementation.

## ACKNOWLEDGEMENTS

One of the authors, T. Somanathan, thanks Central Instrumentation Laboratory (CIL), Vels Institute of Science, Technology and Advanced Studies, for providing the instrumentation facilities.

## CONFLICT OF INTEREST

The authors declare that there is no conflict of interests regarding the publication of this article.

## REFERENCES

1. A. Venkataraman, E.V. Amadi, Y. Chen and C. Papadopoulos, *Nanoscale Res. Lett.*, **14**, 220 (2019); <https://doi.org/10.1186/s11671-019-3046-3>
2. L.M. Esteves, H.A. Oliveira and F.B. Passos, *J. Ind. Eng. Chem.*, **65**, 1 (2018); <https://doi.org/10.1016/j.jiec.2018.04.012>
3. M. Li, Z. Li, Q. Lin, J. Cao, F. Liu and S. Kawi, *Chem. Eng. J.*, **431**, 133970 (2022); <https://doi.org/10.1016/j.cej.2021.133970>
4. S.-Y. Ahn, W.-J. Jang, J.-O. Shim, B.-H. Jeon and H.-S. Roh, *Catal. Rev.*, **66**, 1316 (2023); <https://doi.org/10.1080/01614940.2022.2162677>
5. P. Moodley, J. Loos, J.W. Niemantsverdriet and P.C. Thune, *Carbon*, **47**, 2002 (2009); <https://doi.org/10.1016/j.carbon.2009.03.046>
6. S. Górecka, K. Pacultová, K. Górecki, A. Smýkalová, K. Pamin and L. Obalová, *Catalysts*, **10**, 153 (2020); <https://doi.org/10.3390/catal10020153>
7. X. Chen, Z. Zhao, S. Liu, J. Huang, J. Xie, Y. Zhou, Z. Pan and H. Lu, *J. Rare Earths*, **38**, 175 (2020); <https://doi.org/10.1016/j.jre.2019.01.010>
8. N.T. Nivangune, V.V. Ranade and A.A. Kelkar, *Catal. Lett.*, **147**, 2558 (2017); <https://doi.org/10.1007/s10562-017-2146-x>
9. T. Somanathan and A. Pandurangan, *N. Carbon Mater.*, **25**, 175 (2010); [https://doi.org/10.1016/S1872-5805\(09\)60024-X](https://doi.org/10.1016/S1872-5805(09)60024-X)
10. D. Manikandan, T. Somanathan and J. Phy, *J. Phys. Conf. Ser.*, **2801**, 012008 (2024); <https://doi.org/10.1088/1742-6596/2801/1/012008>
11. K. Abinaya, S.K. Rajkishore, A. Lakshmanan, P. Dhananchezhian, R. Anandham and M. Praghadeesh, *J. Appl. Nat. Sci.*, **13**, 1151 (2021); <https://doi.org/10.31018/jans.v13i4.2916>
12. A. Yahyazadeh, S. Nanda and A.K. Dalai, *Reactions*, **5**, 429 (2024); <https://doi.org/10.3390/reactions5030022>
13. Z. Gholami and G. Luo, *Ind. Eng. Chem. Res.*, **57**, 8871 (2018); <https://doi.org/10.1021/acs.iecr.8b01343>
14. T. Somanathan and A. Pandurangan, *Nano-Micro Lett.*, **2**, 204 (2010); <https://doi.org/10.1007/BF03353642>
15. T.N. Suresh and T. Somanathan, *Mater. Today Proc.*, **46**, 4187 (2021); <https://doi.org/10.1016/j.matpr.2021.02.755>